Int. J. Fuzzy Syst. (2015) 17(2):353–364
DOI 10.1007/s40815-015-0039-y

A Blind Super-Resolution Reconstruction Method Considering Image Registration Errors

Hongyan Zhang[1] · Liangpei Zhang[1] · Huanfeng Shen[2]

Received: 8 September 2014 / Revised: 1 December 2014 / Accepted: 25 March 2015 / Published online: 3 May 2015

Abstract Super-resolution (SR) image reconstruction refers to a process that produces a high-resolution (HR) image from a sequence of low-resolution images that are noisy, blurred, and downsampled. Blind SR is often necessary when the blurring function is unknown. In this paper, to reduce registration errors, we present a new joint maximum a posteriori (MAP) formulation to integrate image registration into blind image SR reconstruction. The formulation is built upon the MAP framework, which judiciously combines image registration, blur identification, and super-resolution. A cyclic coordinate descent optimization procedure is developed to solve the MAP formulation, in which the registration parameters, blurring function, and HR image are estimated in an alternative manner, given the two others, respectively. The proposed algorithm is tested using simulated as well as real-life images. The experimental results indicate that the proposed algorithm has considerable effectiveness in terms of both quantitative measurements and visual evaluation.

Keywords Joint estimation · Maximum a posteriori (MAP) · Image registration · Blur identification · Super-resolution

✉ Hongyan Zhang
zhanghongyan@whu.edu.cn

[1] State Key Laboratory of Information Engineering in Surveying, Mapping, and Remote Sensing, and Collaborative Innovation Center for Geospatial Technology, Wuhan University, Wuhan, People's Republic of China

[2] School of Resource and Environmental Sciences, Wuhan University, Wuhan, People's Republic of China

1 Introduction

Super-resolution (SR) image reconstruction refers to a process that produces a high-resolution (HR) image from a sequence of observed low-resolution (LR) images that are noisy, blurred, and downsampled [1, 2]. Image SR has a variety of applications, including remote sensing [3, 4], video frame freezing, medical diagnostics [5], and military information gathering, etc. The SR problem was first proposed by Tsai and Huang [6] in the frequency domain. They proposed a formulation for the reconstruction of a HR image from a set of undersampled, aliased but noise-free LR images. Their formulation was extended by Kim et al. [7] to consider observation noise as well as the effects of spatial blurring. Then, Kim and Su [8] extended their work by considering different blurs for each LR image. In the spatial domain, typical reconstruction methods include interpolation [9, 10], iterative back projection (IBP) [11], projection onto convex sets (POCS) [12–14], Bayesian/maximum a posteriori (MAP) [15–18], adaptive filtering [19], and sparse coding [20].

Before SR image reconstruction can be carried out, blur identification must be performed to estimate the blurring functions in the image formation process. The precise estimation of the blurring function is very important for the reconstruction of the HR image [21]. Most of the SR image reconstruction algorithms assume a priori known blur [15–18]. However, in many real applications, this assumption is impractical as it is difficult to predict the blur precisely. Consequently, this motivates the study of blind SR image reconstruction, which is a process to perform HR image reconstruction with limited or no knowledge of the blurring function [22]. A few investigations have been carried out to estimate the HR image and blurring function simultaneously, to reduce the effect of blur estimation error. Authors

in [23–25] proposed blind SR that can handle parametric blur models with one parameter. This restriction is, unfortunately, very limiting for most real applications. To our knowledge, early attempts at theoretical blind SR with an arbitrary blurring function have appeared in [26, 27]. Then, He et al. [22] developed a new soft blur learning scheme, which attempts to integrate the parametric information of the blurring function into the algorithm. Sroubek et al. [28] proposed a unifying method that simultaneously estimates the volatile blurs and HR image without any prior knowledge of the blurs and the original image.

Image registration is another process that must be performed to estimate the subpixel shifts between LR images before image SR reconstruction, and plays a critical role in SR image reconstruction [29, 30]. Due to the presence of aliasing in the captured LR images, most existing registration algorithms for aliased images, such as the algorithms described in [31–33], still experience subpixel errors [34]. In the case of non-blind SR where blurring functions are assumed known, many works have been carried out with the emphasis on reducing the effect of registration errors. The simultaneous image registration and reconstruction approach is a quite important approach. Tom and Katsaggelos [35] developed a simultaneous registration and reconstruction approach, in which they formulated the SR problem in the form of a maximum likelihood problem and solved it using the expectation–maximization algorithm. Hardie et al. [36] developed an approach within the MAP framework to simultaneously estimate the image registration parameters and the HR image. Segall et al. [37, 38] presented a noteworthy approach involving the joint estimation of dense motion vectors and HR images for compressed video. Woods et al. [39] presented complex stochastic methods in which the parameters of registration, noise and image statistics are estimated jointly based on the available observations. In [40], Chung et al. proposed a nonlinear cost function, and estimated the registration parameters and the HR image using the Gauss–Newton method. Considering a more generic motion model that includes both translation and rotation, He et al. [34] proposed an iterative scheme based on a non-linear least squares method to estimate the motion parameters and the HR image simultaneously. More recently, Tian and Yap presented a new framework for joint image registration and HR image reconstruction from multiple LR observations with zooming motion.

While in the case of blind SR, there are few reconstruction methods considering registration errors. The conventional blind SR algorithms are performed in two disjoint stages, namely, (1) image registration from LR images, followed by (2) simultaneous estimation of both the HR image and blurring function. Generally speaking, these blind SR algorithms ignore registration errors and assume that the estimated motion parameters of existing registration methods are error free. Obviously, this assumption is impractical in many real applications. Thus, the registration errors will affect the subsequent blind SR image reconstruction to certain extent.

In view of this, this paper proposes a new blind SR reconstruction method considering image registration errors, which establishes a MAP framework for joint image registration, blur identification, and HR image reconstruction. As image registration, blur identification, and SR reconstruction are mutually interdependent and influence each other, an ideal approach is to address them simultaneously. To the best of our knowledge, to date, only two among these three processes have been simultaneously addressed, such as the joint estimation of image registration and reconstruction [30, 34–40] and that of arbitrary blur and image reconstruction [22, 26–28]. The main contribution of this paper is that we integrate image registration into blind SR image reconstruction. Thus, the registration information is iteratively updated along with the progressively estimated blurring function, and HR image, in a cyclic manner. This is more promising as more accurate registration parameters can be determined, thereby improving the performance of the blur identification and SR reconstruction. This algorithm reinforces the interdependence of the registration parameters, blurring function, and HR image in a mutually beneficial manner. Experimental results show that the proposed joint method is effective in performing image registration, blur identification, and SR reconstruction for simulated, as well as real-life images.

The remainder of the paper is organized as follows. In Sect. 2, the SR observation model is described. The joint MAP estimation problem is formulated in Sect. 3. In Sect. 4, the joint optimization procedure to solve the registration parameters, blurring function, and HR image is presented. Experimental results are provided in Sect. 5, and Sect. 6 concludes the paper.

2 Observation Model

The image observation model is employed to relate the desired referenced HR image to the observed LR images. Typically, the imaging process involves warping, followed by blurring and downsampling to generate LR images from the HR image. Let the underlying HR image be denoted in the vector form by $\mathbf{z} = [z_1, z_2, \ldots, z_{L_1N_1 \times L_2N_2}]^T$, where $L_1N_1 \times L_2N_2$ is the HR image size. Letting L_1 and L_2 denote the downsampling factors in the horizontal and vertical directions, respectively, each observed LR image has the size $N_1 \times N_2$. Thus, the LR image can be represented as $\mathbf{g}_k = \left[g_{k,1}, g_{k,2}, \ldots, g_{k,N_1 \times N_2}\right]^T$, where $k = 1, 2, \ldots, P$, with P being the number of LR images. Assuming that

each observed image is contaminated by additive noise, the observation model can be represented as [1]

$$\mathbf{g}_k = \mathbf{D}\mathbf{B}_k\mathbf{M}_k(s)\mathbf{z} + \mathbf{n}_k, \tag{1}$$

where $\mathbf{M}_k(s)$ is the warp matrix with the size of $L_1N_1L_2N_2 \times L_1N_1L_2N_2$, s represents the registration information, $\mathbf{B}_k$ represents the camera blur matrix also of size $L_1N_1L_2N_2 \times L_1N_1L_2N_2$, $\mathbf{D}$ is a $N_1N_2 \times L_1N_1L_2N_2$ downsampling matrix, and $\mathbf{n}_k$ represents the $N_1N_2 \times 1$ noise vector. Figure 1 illustrates (1).

Similar to most work on SR [1, 22], it is assumed in this paper that the imaging blur is spatial shift-invariant and the warping between different LR images is translational. Using the commutative property of convolution [41], (1) may be written as

$$\mathbf{g}_k = \mathbf{D}\mathbf{M}_k(s)\mathbf{B}_k\mathbf{z} + \mathbf{n}_k = \mathbf{D}\mathbf{M}_k(s)\mathbf{Z}\mathbf{b}_k + \mathbf{n}_k, \tag{2}$$

where $\mathbf{B}_k\mathbf{z}$, the blurry version of the HR image, can also be written as $\mathbf{Z}\mathbf{b}_k$, by introducing a $L_1N_1L_2N_2 \times r_1r_2$ matrix $\mathbf{Z}$, which is constructed from image $\mathbf{z}$. $\mathbf{b}_k$ is the blur kernel with the size of $r_1r_2 \times 1$; here $r_1 \times r_2$ represents the support of the blurring function. Let the full set of P LR images, blurring functions and registration parameters be denoted by $\mathbf{g} = \{\mathbf{g}_1, \mathbf{g}_2, \ldots, \mathbf{g}_P\}$, $\mathbf{b} = \{\mathbf{b}_1, \mathbf{b}_2, \ldots, \mathbf{b}_P\}$, and $\mathbf{s} = \{\mathbf{s}_1, \mathbf{s}_2, \ldots, \mathbf{s}_P\}$, respectively. By stacking (2), we get

$$\mathbf{g} = \mathbf{D}\mathbf{M}(s)\mathbf{B}\mathbf{z} + \mathbf{n} = \mathbf{D}\mathbf{M}(s)\mathbf{Z}\mathbf{b} + \mathbf{n}. \tag{3}$$

3 Problem Formulation

The purpose is to realize the joint MAP estimate of HR image $\mathbf{z}$, blurring functions $\mathbf{b}$, and registration information $\mathbf{s}$, given the observed LR images $\mathbf{g}$. The estimate can be computed by

$$\hat{\mathbf{z}}, \hat{\mathbf{b}}, \hat{\mathbf{s}} = \arg\max\{p(\mathbf{z}, \mathbf{s}, \mathbf{b}|\mathbf{g})\}. \tag{4}$$

Applying Bayes' rule, after some manipulation, we can get

$$\begin{aligned}\hat{\mathbf{z}}, \hat{\mathbf{b}}, \hat{\mathbf{s}} = \arg\max\{&\log p(\mathbf{g}|\mathbf{z}, \mathbf{b}, \mathbf{s}) \\ &+ \log p(\mathbf{z}) + \log p(\mathbf{b}) + \log p(\mathbf{s})\}.\end{aligned} \tag{5}$$

The central task then becomes constructing the four probability density functions (PDFs) so as to enable the MAP estimation. The PDF $p(\mathbf{g}|\mathbf{z}, \mathbf{b}, \mathbf{s})$ provides a measure of the conformance of the estimated image to the observed images, according to the image observation model. It is determined by the probability density of the noise vector in (3). Assuming that the noise $\mathbf{n}$ is additive white Gaussian noise (AWGN) with variance σ^2, the likelihood $p(\mathbf{g}|\mathbf{z}, \mathbf{b}, \mathbf{s})$ can be given by

$$p(\mathbf{g}|\mathbf{z}, \mathbf{b}, \mathbf{s}) = \frac{1}{C_1}\exp\left(-\frac{\|\mathbf{g} - \mathbf{D}\mathbf{B}\mathbf{M}(s)\mathbf{z}\|^2}{2\sigma^2}\right), \tag{6}$$

where C_1 is a constant.

The PDF $p(\mathbf{z})$ is the image prior, which imposes the spatial constraints on the image. For the image prior term, the Laplacian prior [17, 39] and the Gauss–Markov prior [36] are commonly employed. A common criticism of these regularization methods is that detailed information in the estimates tends to be overly smoothed [32]. Therefore, an edge-preserving Huber–Markov image prior is employed in this paper. This prior can effectively preserve the edge and detailed information in the image [16]. The Huber–Markov prior has the following form:

$$p(\mathbf{z}) = \frac{1}{C_2}\exp\left(-\frac{1}{2\lambda_1}\sum_{x,y}\sum_{c\in C}\rho(d_c(\mathbf{z}_{x,y}))\right). \tag{7}$$

In this expression, C_2 is a constant, c is a clique within the set of all image cliques C, and the quantity $d_c(\mathbf{z}_{x,y})$ is a spatial activity measure of pixel $\mathbf{z}_{x,y}$, which is often formed by first- or second-order differences. The potential function $\rho(i)$ is the Huber function, defined as

$$\rho(i) = \begin{cases} i^2 & |i| \le \mu \\ 2\mu|i| - \mu^2 & |i| > \mu \end{cases} \tag{8}$$

where μ is a threshold parameter separating the quadratic and linear regions [16]. As for the function $d_c(\mathbf{z}_{x,y})$, we compute the following finite second-order differences in four adjacent cliques for every location (x, y) in the SR image:

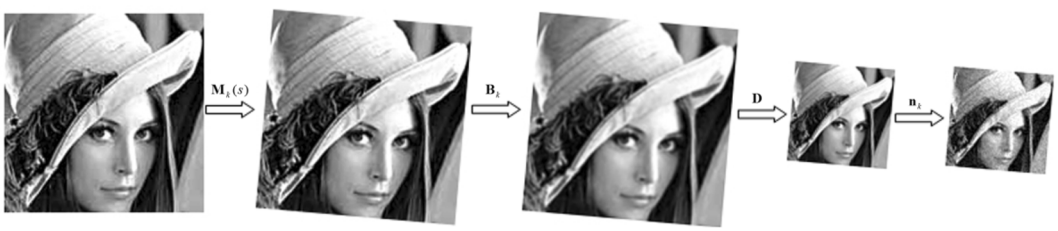

Fig. 1 Block diagram illustration of the observation model (1), where the desired HR image is at the extreme *left*, and the observed image at the extreme *right* [18]

$$
\begin{aligned}
d_c^1(\mathbf{z}_{x,y}) &= \mathbf{z}_{x-1,y} - 2\mathbf{z}_{x,y} + \mathbf{z}_{x+1,y} \\
d_c^2(\mathbf{z}_{x,y}) &= \mathbf{z}_{x,y-1} - 2\mathbf{z}_{x,y} + \mathbf{z}_{x,y+1} \\
d_c^3(\mathbf{z}_{x,y}) &= \frac{1}{\sqrt{2}}\left[\mathbf{z}_{x-1,y-1} - 2\mathbf{z}_{x,y} + \mathbf{z}_{x+1,y+1}\right] \cdot \\
d_c^4(\mathbf{z}_{x,y}) &= \frac{1}{\sqrt{2}}\left[\mathbf{z}_{x-1,y+1} - 2\mathbf{z}_{x,y} + \mathbf{z}_{x+1,y-1}\right]
\end{aligned} \tag{9}
$$

The PDF $p(\mathbf{b})$ is the blur function prior, which imposes the spatial constraints in the blur domain. As the blurring function is unknown, we should take the piecewise smoothness property of the blurring function into consideration. In this paper, the following Laplacian prior model [25, 27] is used:

$$
p(\mathbf{b}) = \frac{1}{C_3}\exp\left(-\lambda_2\|\mathbf{Qb}\|^2\right), \tag{10}
$$

where λ_2 is a parameter that controls the contribution of the blurring function prior model, and $\mathbf{Q}$ is a 2-D Laplacian here.

The choice of a prior model for the registration parameters is highly application specific [36]. If there are relatively few registration parameters to estimate, a "no preference" prior can yield a useful solution. Considering that a translational motion model is used in this paper, there are only two registration parameters for each LR image, and a "no preference" prior is used here. Thus, the estimation of the registration parameters reduces to an ML estimate [36].

Substituting (6), (7), and (10) into (5), after some manipulation, the minimization cost function is obtained in (11)

$$
\begin{aligned}
\hat{\mathbf{z}}, \hat{\mathbf{b}}, \hat{\mathbf{s}} = \arg\min\Bigg\{ &\|\mathbf{g} - \mathbf{DM}(s)\mathbf{Bz}\|^2 + \alpha \sum_{x,y}\sum_{c\in C}\rho(d_c(\mathbf{z}_{x,y})) \\
&+\beta\|\mathbf{Qb}\|^2\Big\}.
\end{aligned} \tag{11}
$$

This cost function is used in the optimization procedure introduced subsequently.

4 Optimization Procedure

It is noted that the cost function (11), as a joint function of three sets of variables, is not convex. Therefore, a cyclic coordinate descent optimization procedure is developed to solve the unknowns. The registration parameters, blurring function, and HR image are found in an alternate manner, given the two others, respectively.

4.1 Updating Unknowns

Given the full set of registration parameters $\mathbf{s}$ and blurring functions $\mathbf{b}$, the desired HR image $\mathbf{z}$ can be updated by minimizing the following cost function:

$$
E_1(\mathbf{z}) = \|\mathbf{g} - \mathbf{DM}(s)\mathbf{Bz}\|^2 + \alpha \sum_{x,y}\sum_{c\in C}\rho(d_c(\mathbf{z}_{x,y})), \tag{12}
$$

which is composed of the two terms in (11) that contain the sole unknown quantity $\mathbf{z}$. This is a regularized optimization problem. To solve the desired HR image $\mathbf{z}$, we use the method of conjugate gradients.

Given the estimate of HR image $\mathbf{z}$ and registration information $\mathbf{s}$, the cost function to estimate the blurring function $\mathbf{b}$ is given by:

$$
E_2(\mathbf{b}) = \|\mathbf{g} - \mathbf{DM}(s)\mathbf{Zb}\|^2 + \beta\|\mathbf{Qb}\|^2. \tag{13}
$$

It is common to assume that the blurring function is positive and preserves image brightness, so the blurring function should satisfy the following constraints:

$$
\mathbf{b}_k(i,j) \geq 0 \quad \text{and} \quad \sum\nolimits_{i,j} \mathbf{b}_k(i,j) = 1. \tag{14}
$$

Therefore, we can restrict the intensity values of the blurring function between 0 and 1. In order to enforce these bounds, we solve (13) as a constrained optimization problem. Constrained optimization problems are more computationally demanding, but we can afford it in this case since the size of the blurring function is much smaller than the size of HR image.

Given the estimate of the HR image $\mathbf{z}$ and blurring function $\mathbf{b}$, the cost function to estimate the registration information $\mathbf{s}$ can be given as

$$
E_3(\mathbf{s}) = \|\mathbf{g} - \mathbf{DM}(s)\mathbf{Bz}\|^2. \tag{15}
$$

A search is required to minimize (15) with respect to $\mathbf{s}$. Pyramidal search strategies designed for traditional block matching can be employed here [36]. As opposed to the two-stage blind SR methods that perform registration on the LR images in the first stage, the image registration is performed iteratively here, using the progressively estimated HR image and blurring function. It is believed that more precise registration parameters can be obtained, thereby enhancing the performance of the HR reconstruction and blur identification.

4.2 Initialization

Before updating all these unknowns, the HR image, registration information, and blurring function must be initiated. The initial HR image is obtained using bicubic interpolation of the reference LR image. The registration parameters are initiated by implementing an existing registration algorithm, such as the parameter model-based image registration algorithm [32]. The initial estimate of the blurring function is obtained using the method described in [27], which should not be far away from the real values. The two regularization parameters in (11) are

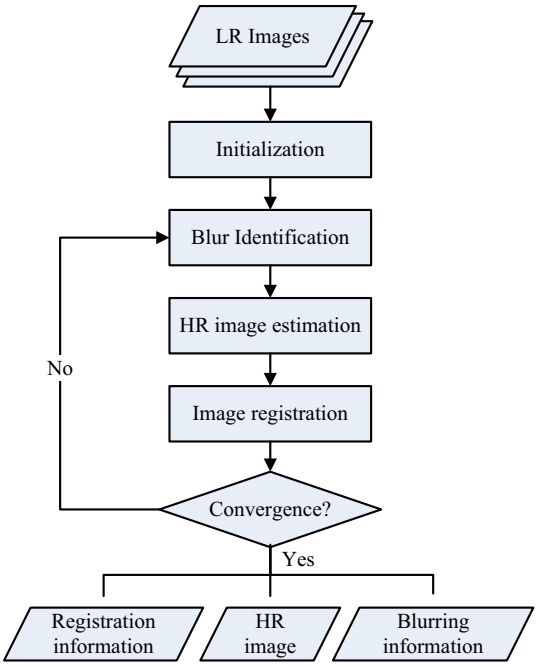

Fig. 2 Diagram of the joint MAP algorithm

determined heuristically, according to quantitative evaluations or visual assessments in our experiments. That is, a set of properly chosen parameter values are tested, and the values which correspond to the optimal quantitative evaluations and visual assessments are selected.

A block diagram of the whole optimization procedure is shown in Fig. 2. The number of iteration ($N = 10$) is used as a stopping criterion in this paper.

5 Experimental Results

In this section, we illustrate the performance of the proposed method on two different sets of data: simulated and real-life images. To evaluate the performance, the normalized mean-square error (NMSE) and peak signal-to-noise ratio (PSNR) [42, 43] were employed as quantitative measures for the estimated registration information, blurring function, and HR image in the simulated experiments. Generally speaking, a good algorithm is reflected by low NMSE and high PSNR.

5.1 Simulated Images

We conducted simulation experiments to perform blind SR on multiple noisy LR images with different blur levels. The "cameraman" image in Fig. 3a was selected as the test image. To generate the LR images, the HR image was first shifted with 0, 1, 2, or 3 HR pixels in the horizontal and vertical directions, respectively, and then blurred with a symmetric Gaussian blur before downsampling by a decimation factor of 4. The LR images were further degraded by AWGN, yielding a signal-to-noise ratio (SNR) of 30 dB. We experiment with Gaussian blurs of variances 0.75, 1.0,, and 1.5 and try to estimate the blurring functions, assuming that the support of the PSF has been known. For each level of Gaussian blur, 16 synthetic degraded images are generated and used by a resolution enhancement factor of 4 in this experiment. The two-stage disjoint blind image SR method, which doesn't consider image registration errors, was utilized as the benchmark algorithm of the proposed method. In addition, the image SR reconstruction with the exactly known blur and registration information, was also applied to the observed LR images to give full comparisons with the experimental results of the proposed method. The two-stage disjoint blind SR method was implemented with two steps of independent image registration procedure over the LR observed images and solving the MAP cost function in (11) with respect to the HR image and blurring function, iteratively, which is very similar to the methods in [20], except for the types of blurring function and image priors utilized to ensure the fairness of comparisons. Our proposed method was run based on the procedure shown in Fig. 2. We performed image registration using the translational parameter model-based image registration algorithm, which is a special case of the six-parameter affine model in [32]. SR reconstruction with known blur and registration information was implemented by minimizing the cost function in (12), assuming that the blur and registration information were exactly known.

The NMSE of the registration information under different Gaussian blur levels is given in Table 1. Comparing the image registration information obtained with predefined image registration method [32], the proposed method updates the registration information using the progressively estimated blurring function with the HR image and greatly improves image registration accuracy. Tables 2 and 3, respectively, show the NMSE of the estimated blurring function and PSNR of the reconstructed HR images under different Gaussian blur levels. From these tables, it is clearly observed that the proposed method achieves a more accurate blurring function and better reconstruction results than the two-stage disjoint blind SR method without considering image registration errors. These observations further reconfirm the NMSE results of the registration information obtained with the proposed method with considering image registration errors in the blurring information estimation and image reconstruction processes from another perspective. Comparing our results with those of the two-stage disjoint blind SR method, it is found that the improvement of image registration has a direct effect on the blur identification and SR reconstruction, thereby

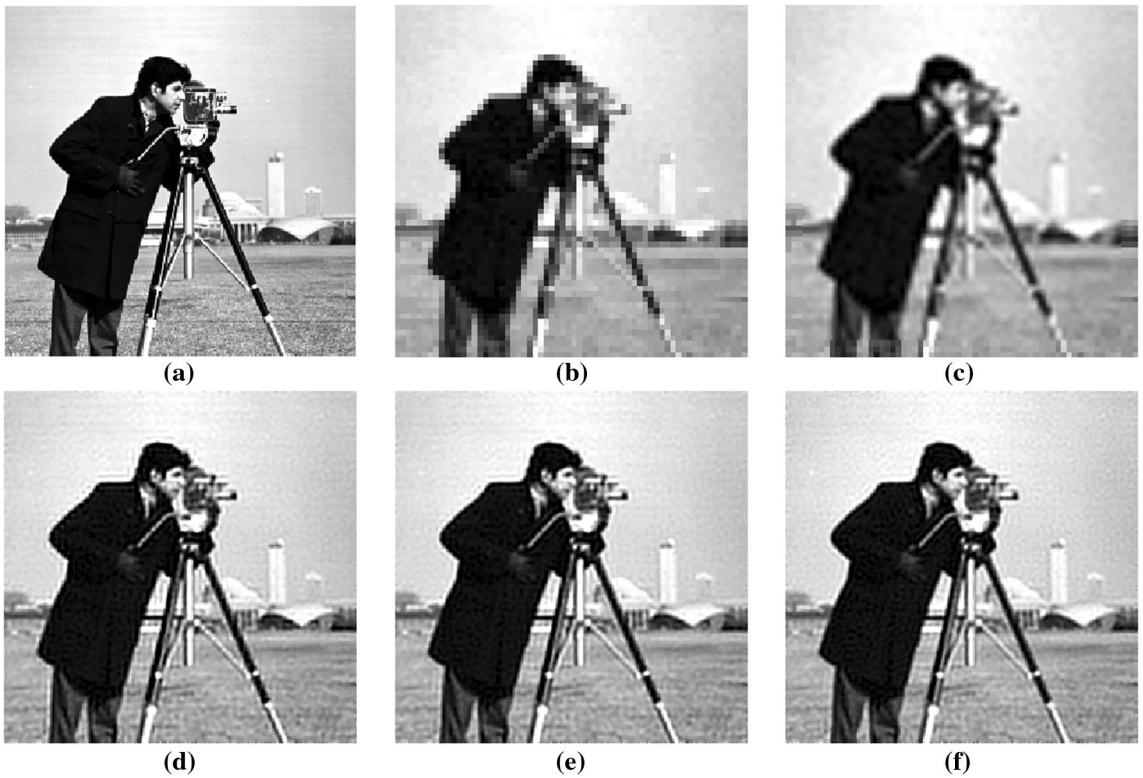

Fig. 3 SR reconstruction result of LR images with Gaussian blur of variance 0.75. **a** Original HR image, **b** the referenced LR image, **c** bicubic interpolation, **d** two-stage disjoint blind SR method without considering image registration errors, and **e** proposed method and **f** SR reconstruction result with exactly known blur and registration information

Table 1 NMSE of the registration information under different Gaussian blur levels

Methods	Variance = 0.75	Variance = 1.0	Variance = 1.5
Two-stage disjoint blind SR method without considering registration errors	0.7831	0.7850	0.7976
The proposed method	0.0458	0.0378	0.0351

Table 2 NMSE of the blurring function under different Gaussian blur levels

Methods	Variance = 0.75	Variance = 1.0	Variance = 1.5
Two-stage disjoint blind SR method without considering registration errors	1.00	0.95	0.89
The proposed method	0.64	0.60	0.54

Table 3 PSNR of the reconstructed HR image under different Gaussian blur levels

Methods	Variance = 0.75	Variance = 1.0	Variance = 1.5
Bicubic interpolation	22.56	22.53	22.46
Two-stage disjoint blind SR method without considering registration errors	25.71	25.55	25.21
The proposed method	26.04	25.79	25.36
SR reconstruction with exactly known blur and registration information	26.15	25.85	25.47

improving the accuracy of estimated blur function and the quality of the reconstructed HR image.

Now the emphasis is on the evaluation and analysis of the reconstructed HR images. Here we compared the reconstructed HR image results of the three sets of LR images, to validate the performance of the proposed method under different Gaussian blur levels. The threshold parameter μ in (8) is set as 5 in all three experiments. The SR reconstruction results with Gaussian blurs of variances 0.75, 1.0, and 1.5 are illustrated in Figs. 3, 5, and 7, respectively. To facilitate a better comparison, a region of each is shown in detail in Figs. 4, 6, and 8, respectively. Comparing the reconstruction results in Figs. 3, 4, 5, 6, 7, and 8, it is obviously observed that the image reconstructed by the two-stage disjoint blind SR method has much better visual quality than the interpolated image. However, artifacts are displayed around the edges because of the existence of the image registration errors, such as at the right elbow of the cameraman. The proposed method makes an obvious improvement best described as a suppression of these artifacts by considering the image registration errors in the blurring information estimation and image reconstruction processes, and obtains a very close result to the SR reconstruction result with exactly known blur and registration information. From the quantitative comparison results given in Table 3, it is observed that quantitative measures agree with the visual evaluation. Evidently, the proposed algorithm outperforms the two-stage disjoint blind SR algorithm, in terms of both the quantitative measurements and visual evaluation, which validate the effectiveness of considering the image registration errors within the proposed image blind SR reconstruction procedure.

5.2 Real-life Images

The real-life images experiment was conducted on the "castle" image sequence. We used four images with image 1 as the referenced image, which is shown in Fig. 9a. The parameter model-based image registration algorithm in [32] was again used to estimate the registration parameters from the LR images. Next, the two-stage disjoint blind SR method without considering image registration errors and our proposed method were run to perform blind image SR reconstruction. Figure 9b–d shows the bicubic interpolated image, the two-stage disjoint blind SR result and the result by the proposed method, respectively. Sampled regions cropped from Fig. 9b–d are depicted in Fig. 10a–c, respectively. The parameters used for this example are set as follows: $\alpha = 0.01$, $\beta = 10{,}000$, and $\mu = 5$. From the figures, it is observed that the considerable clarity of the images has been recovered by both the two-stage disjoint

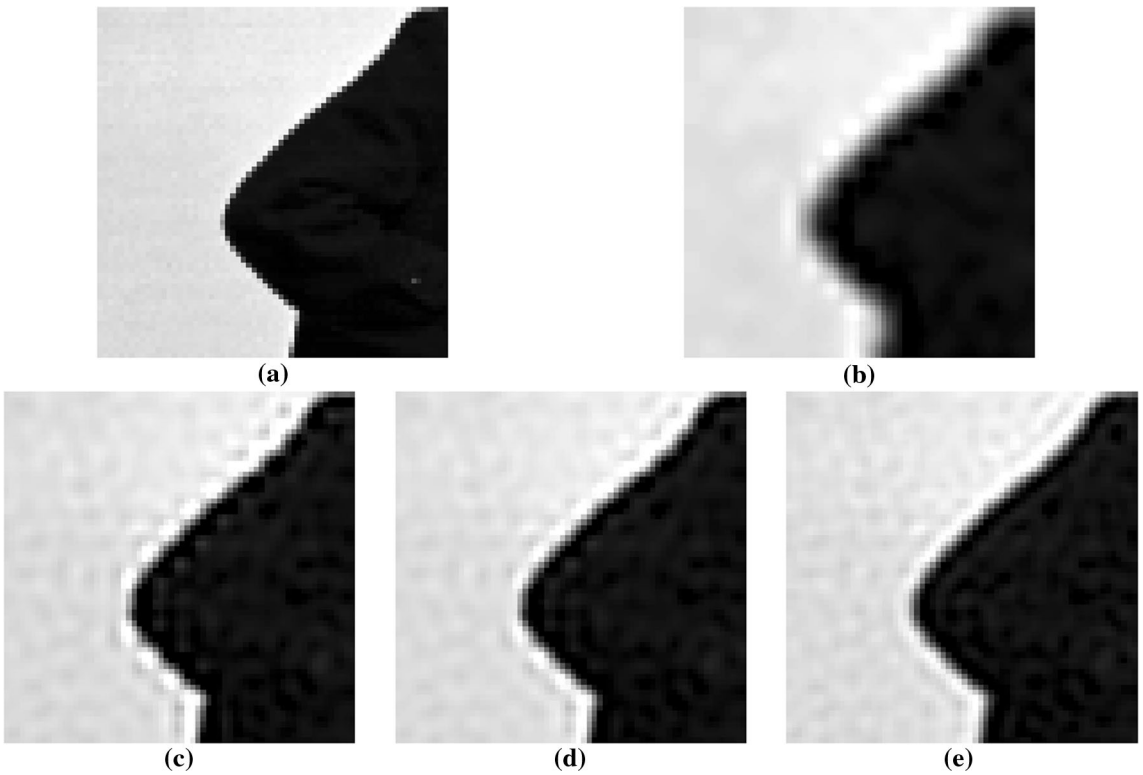

Fig. 4 **a–e** Sampled regions cropped from Fig. 3(a), (c)–(f), respectively

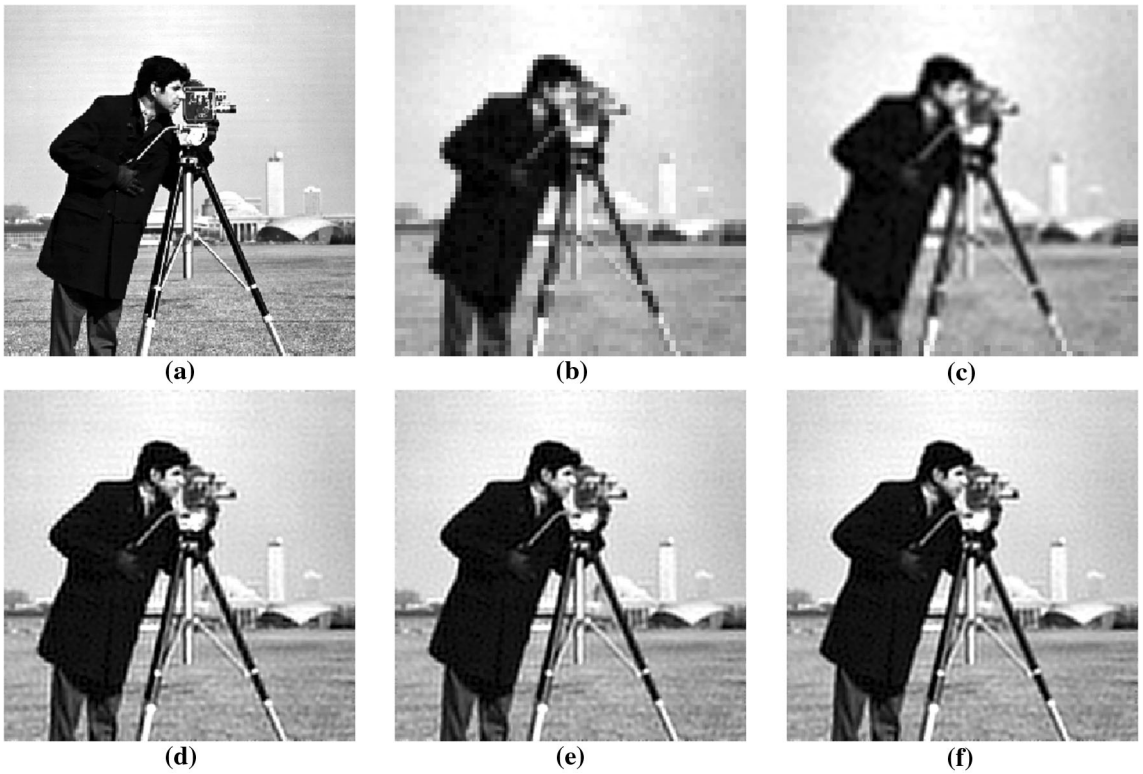

Fig. 5 SR reconstruction result of LR images with Gaussian blur of variance 1.0. **a** Original HR image, **b** the referenced LR image, **c** bicubic interpolation, **d** two-stage disjoint blind SR method without considering image registration errors, and **e** proposed method and **f** SR reconstruction result with exactly known blur and registration information

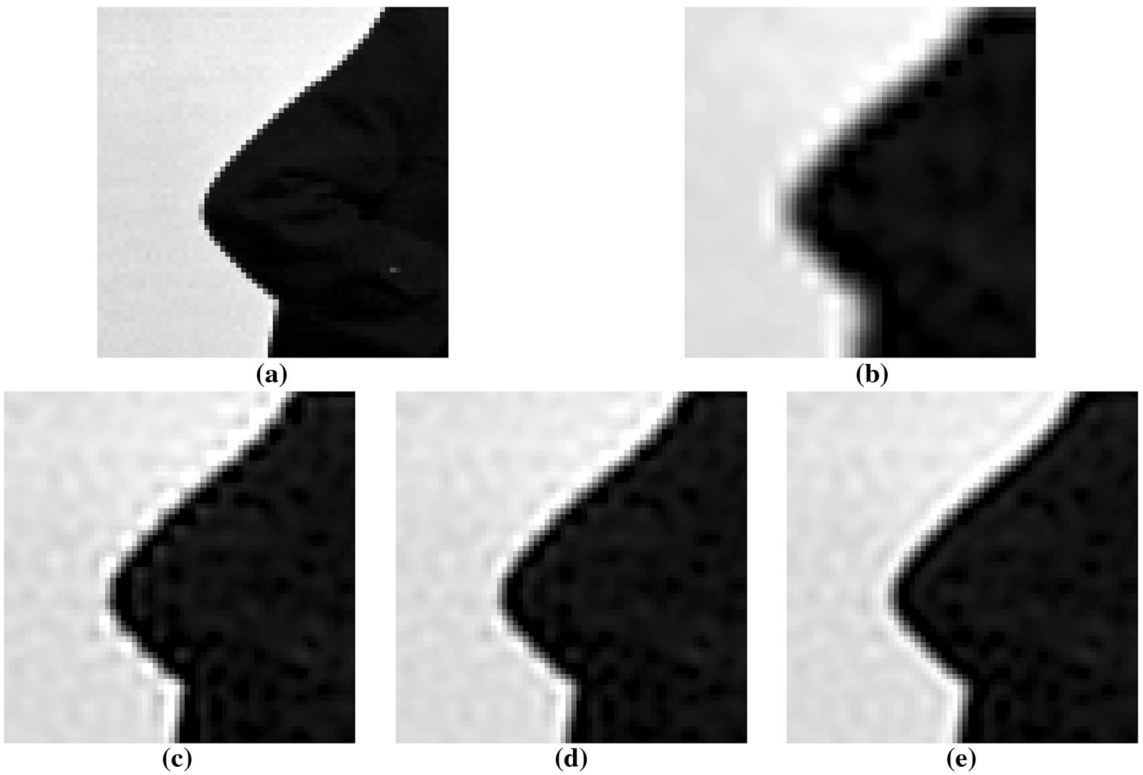

Fig. 6 **a–e** Sampled regions cropped from Fig. 5(a), (c)–(f), respectively

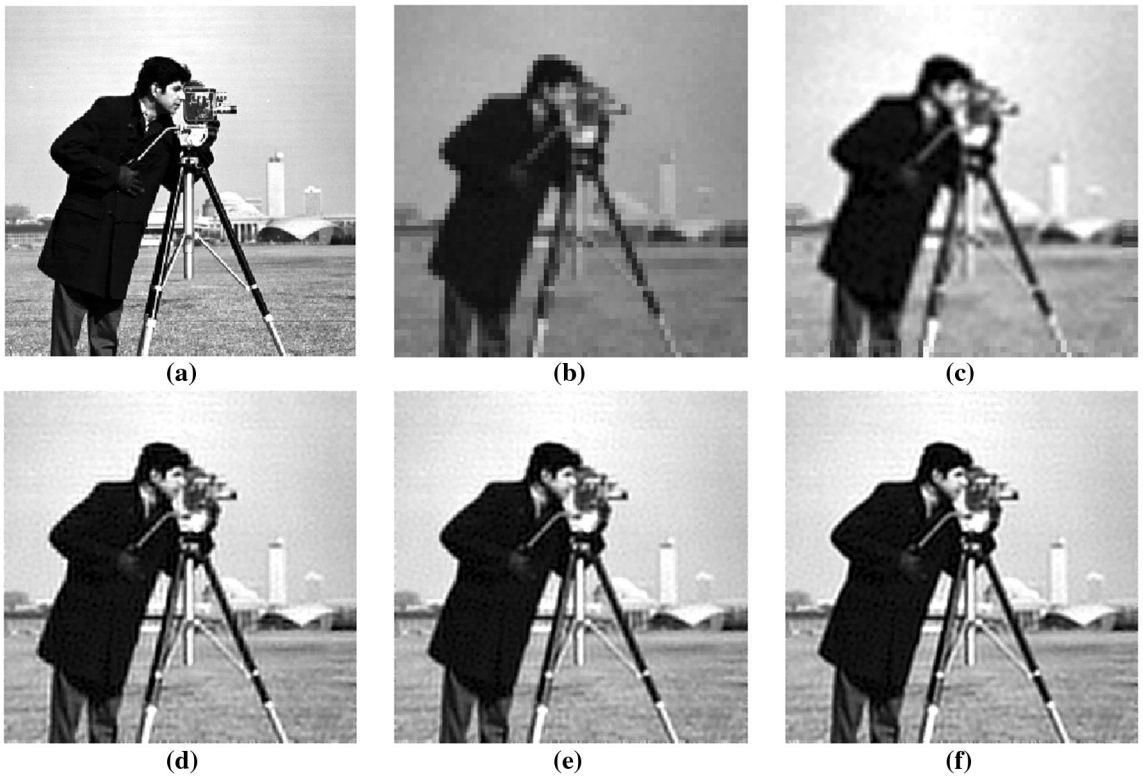

Fig. 7 SR reconstruction result of LR images with Gaussian blur of variance 1.5. **a** Original HR image, **b** the referenced LR image, **c** bicubic interpolation, **d** two-stage disjoint blind SR method without considering image registration errors, and **e** proposed method and **f** SR reconstruction result with exactly known blur and registration information

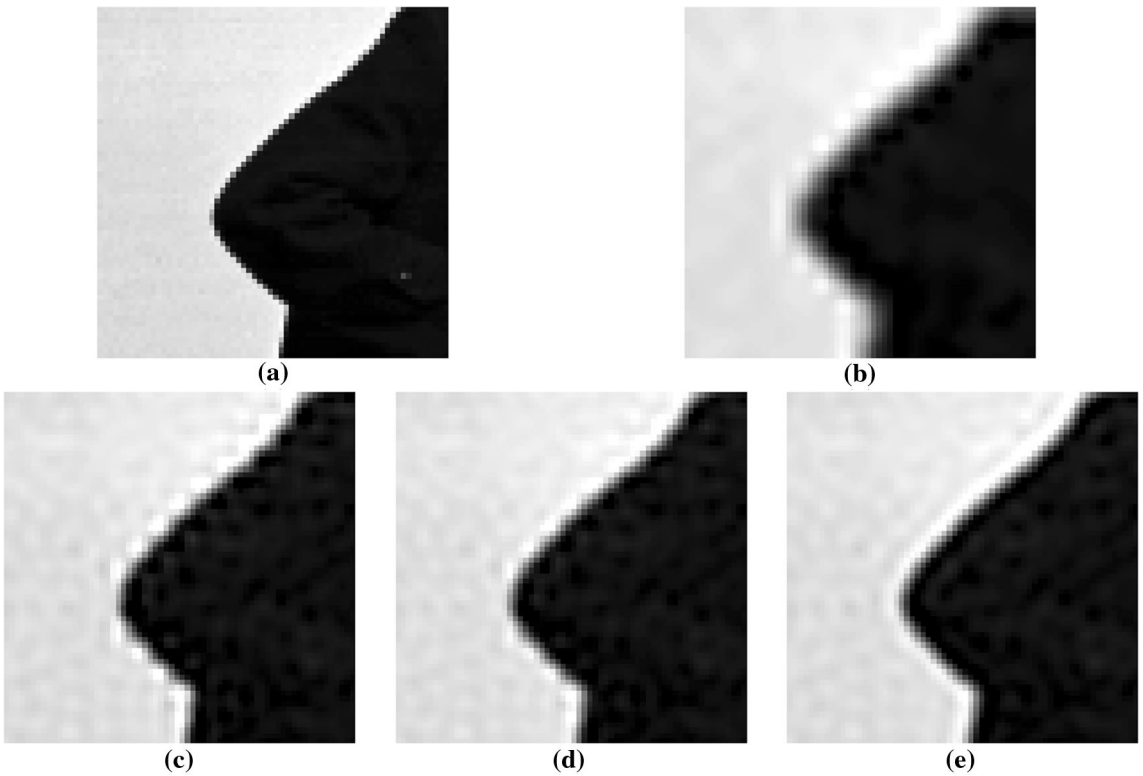

Fig. 8 **a–e** Sampled regions cropped from Fig. 7(a), (c)–(f), respectively

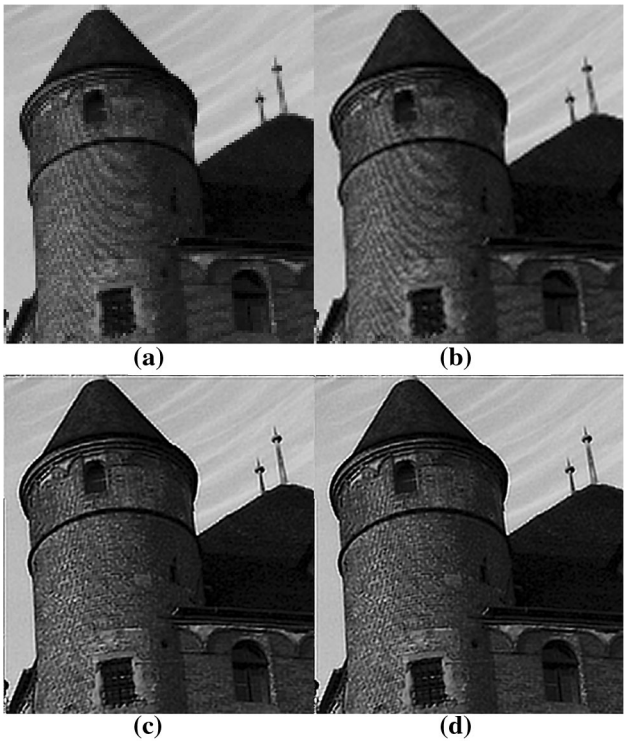

Fig. 9 Blind SR reconstruction of the "castle" image sequence. **a** The referenced LR image, **b** bicubic interpolation, **c** two-stage disjoint blind SR method without considering image registration errors, and **d** the proposed method

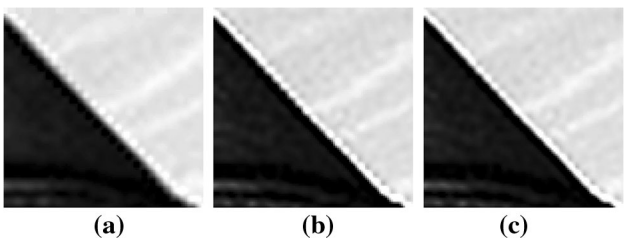

Fig. 10 a–c Sampled regions cropped from Fig. 13(b)–(d), respectively

blind SR method and the proposed method. Further, it can be seen that the result by our proposed method has fewer artifacts than in the two-stage disjoint blind SR method, in particular near the edges. Comparison reveals that our approach is superior in handling real-life blind image SR, as it is able to estimate image registration parameters accurately, leading to superior blur identification and HR image reconstruction.

6 Conclusion

This paper presents a new blind SR reconstruction method by integrating image registration into blind image SR reconstruction to reduce the effect of registration errors, and then a cyclic coordinate descent optimization procedure is developed to solve the formulation. As opposed to the two-stage blind SR methods that perform image registration and blind SR reconstruction as disjoint processes, the new framework enables image registration, blur identification, and HR image reconstruction to be estimated and improved progressively. The advantage of this algorithm is that image registration information, blurring function, and the HR image can benefit each other. The proposed algorithm was tested on simulated, as well as real-life images. The experimental results validated that registration parameters, blurring information, and the HR image can be noticeably improved by implementing this algorithm. Nevertheless, there may still be room for improvements to our optimal method, to increase computational efficiency. Using more robust prior models for the blurring function (e.g., the best-fit parametric blur model [22]) may further improve the SR results. These will be addressed in our future work.

Acknowledgments This work was supported in part by the National Basic Research Program of China (973 Program) under Grant 2011CB707105, by the 863 Program under Grant 2013AA12A301, and in part by the National Natural Science Foundation of China under Grant 61201342 and Grant 41431175.

References

1. Park, S.C., Park, M.K., Kang, M.G.: Super-resolution image reconstruction: a technical overview. IEEE Signal Process. Mag. **20**(3), 21–36 (2003)
2. Farsiu, S., Robinson, D., Elad, M., Milanfar, P.: Advances and challenges in super-resolution. Int. J. Imaging Syst. Technol. **14**(2), 47–57 (2004)
3. Zhang, H., Yang, Z., Zhang, L., Shen, H.: Super-resolution reconstruction for multi-angle remote sensing images considering resolution differences. Remote Sens. **6**(1), 637–657 (2014)
4. Yang, J., Yu, P., Kuo, B., Su, M.: Nonparametric fuzzy feature extraction for hyperspectral image classification. Int. J. Fuzzy Syst. **12**(3), 208–217 (2010)
5. Lakdashti, A., Moin, M.S., Badie, K.: Reducing the semantic gap of the MRI image retrieval systems using a fuzzy rule based technique. Int. J. Fuzzy Syst. **11**(4), 232–249 (2009)
6. Tsai, R.Y., Huang, T.S.: Multi-frame image restoration and registration. Adv. Comput. Vis. Image Process. **1**, 317–339 (1984)
7. Kim, S.P., Bose, N.K., Valenzuela, H.M.: Recursive reconstruction of high resolution image from noisy undersampled multiframes. IEEE Trans. Acoust. Speech Signal Process. **38**(2), 1013–1027 (1990)
8. Kim, S.P., Su, W.Y.: Recursive high-resolution reconstruction of blurred multiframe images. IEEE Trans. Image Process. **2**(4), 534–539 (1993)
9. Sanchez-Beato, A., Pajares, G.: Noniterative interpolation-based super-resolution minimizing aliasing in the reconstructed image. IEEE Trans. Image Process. **17**, 1817–1826 (2008)
10. Zhou, F., Yang, W., Liao, Q.: Interpolation-based image super-resolution using multi-surface fitting. IEEE Trans. Image Process. **21**(6), 3312–3318 (2012)
11. Irani, M., Peleg, S.: Improving resolution by image registration. CVGIP: Graph Models Image Process. **53**, 231–239 (1991)

12. Stark, H., Oskoui, P.: High-resolution image recovery from image plane arrays, using convex projections. J. Opt. Soc. Am. A **6**, 1715–1726 (1989)
13. Patti, A. J., Sezan, M. I., Tekalp, A. M.: High-resolution image reconstruction from a low-resolution image sequence in the presence of time-varying motion blur. Presented at IEEE international conference on image processing, Austin, TX, USA (1994)
14. Patti, A.J., Sezan, M.I., Tekalp, A.M.: Superresolution video reconstruction with arbitrary sampling lattices and nonzero aperture time. IEEE Trans. Image Process. **6**(8), 1064–1076 (1997)
15. Schultz, R.R., Stevenson, R.L.: Extraction of high-resolution frames from video sequences. IEEE Trans. Image Process. **5**(6), 996–1011 (1996)
16. Zhang, L., Zhang, H., Shen, H., Li, P.: A Super-resolution reconstruction algorithm for surveillance images. Signal Process. **90**(3), 848–859 (2010)
17. Pickup, L. C., Capel, D. P., Roberts, S. J., Zisserman, A.: Bayesian image super-resolution, continued. Adv. Neural Inf. Process. Syst. pp. 1089–1096 (2006)
18. Zhang, H., Shen, H., Zhang, L.: A super-resolution reconstruction algorithm for hyperspectral images. Signal Process. **92**(9), 2082–2096 (2012)
19. Hardie, R.: A fast image super-resolution algorithm using an adaptive Wiener filter. IEEE Trans. Image Process. **16**(12), 2953–2964 (2007)
20. Barzigar, N., Roozgard, A., Verna, P., Cheng, S.: A video super resolution framework using SCoBeP. IEEE Trans. Circuits Syst. Video Technol. (2014). doi:10.1109/TCSVT.2013.2283108
21. He, H., Kondi, L.P.: An image super-resolution algorithm for different error levels per frame. IEEE Trans. Image Process. **15**(3), 592–603 (2006)
22. He, Y., Yap, K.H., Chen, L., Chau, L.P.: A soft MAP framework for blind super-resolution image reconstruction. Image Vis. Comput. **27**, 364–373 (2009)
23. Nguyen, N., Milanfar, P., Golub, G.: Efficient generalized cross-validation with applications to parametric image restoration and resolution enhancement. IEEE Trans. Image Process. **10**(9), 1299–1308 (2001)
24. Woods, N., Galatsanos, N., Katsaggelos, A.: EM-based simultaneous registration, restoration, and interpolation of super-resolved images. Presented at IEEE international conference on image processing, vol. 2, pp. 303–306 (2003)
25. Yang, H., Gao, J., Wu, Z.: Blur identification and image super-resolution reconstruction using an approach similar to variable projection. IEEE Signal Process. Lett. **15**, 289–292 (2008)
26. Yagle, A.: Blind superresolution from undersampled blurred measurements. Presented at advanced signal processing algorithms, architectures, and implementations XIII, vol. 5205, pp. 299–309 (2003)
27. He, H., Kondi, L. P.: A regularization framework for joint blur estimation and super-resolution of video sequences. Presented at IEEE international conference on image processing, Genova (2005)
28. Sroubek, F., Cristóbal, G., Flusser, J.: A unified approach to super-resolution and multichannel blind deconvolution. IEEE Trans. Image Process. **16**(9), 2322–2332 (2007)
29. Shen, H., Zhang, L., Huang, B., Li, P.: A MAP approach for joint motion estimation, segmentation, and super resolution. IEEE Trans. Image Process. **16**(2), 479–490 (2007)
30. Tian, Y., Yap, K.: Joint image registration and super-resolution from low-resolution images with zooming motion. IEEE Trans. Circuits Syst. Video Technol. **23**(7), 1224–1234 (2013)
31. Vandewalle, P., Susstrunk, S., Vetterli, A.: A frequency domain approach to registration of aliased images with application to super-resolution. EURASIP J. Appl. Signal Process. (Article ID 71459) (2006)
32. Ng, M. K., Shen, H., Lam, E., Zhang, L.: A total variation regularization based Super-Resolution Reconstruction Algorithm for Digital Video. EURASIP J. Appl. Signal Process. (Article ID 74585) (2007)
33. Hu, T., Zhang, H., Shen, H., Zhang, L.: Robust registration by rank minimization for multi-angle multi/hyper-spectral remote sensing imagery. IEEE J. Sel. Top. Appl. Earth Obs. Remote Sens. **7**(6), 2443–2457 (2014)
34. He, Y., Yap, K.H., Chen, L., Chau, L.P.: A nonlinear least square technique for simultaneous image registration and super-resolution. IEEE Trans. Image Process. **16**(11), 2830–2840 (2007)
35. Tom, B. C., Katsaggelos, A. K.: Reconstruction of a high-resolution image by simultaneous registration, restoration, and interpolation of low-resolution images. Presented at IEEE international conference on image processing, Washington, DC (1995)
36. Hardie, R.C., Barnard, K.J., Armstrong, E.E.: Joint MAP registration and high-resolution image estimation using a sequence of undersampled images. IEEE Trans. Image Process. **6**(12), 1621–1633 (1997)
37. Segall, C.A., Molina, R., Katsaggelos, A.K.: High-resolution images from low-resolution compressed video. IEEE Signal Process. Mag. **20**(3), 37–48 (2003)
38. Segall, C.A., Katsaggelos, A.K., Molina, R., Mateos, J.: Bayesian resolution enhancement of compressed video. IEEE Trans. Image Process. **13**(7), 898–910 (2004)
39. Woods, N.A., Galatsanos, N.P., Katsaggelos, A.K.: Stochastic methods for joint registration, restoration, and interpolation of multiple undersampled images. IEEE Trans. Image Process. **15**(1), 201–213 (2006)
40. Chung, J., Haber, E., Nagy, J.: Numerical methods for coupled superresolution. Inverse Prob. **22**, 1261–1272 (2006)
41. Elad, M., Hel-Or, Y.: A fast super-resolution reconstruction algorithm for pure translational motion and common space-invariant blur. IEEE Trans. Image Process. **10**(8), 1187–1193 (2001)
42. Zhang, H., He, W., Zhang, L., Shen, H., Yuan, Q.: Hyperspectral image restoration using low-rank matrix recovery. IEEE Trans. Geosci. Remote Sens. **52**(8), 4729–4743 (2014)
43. Jiang, C., Zhang, H., Shen, H., Zhang, L.: Two-step sparse coding for the pan-sharpening of remote sensing images. IEEE J. Sel. Top. Appl. Earth Obs. Remote Sens. **7**(5), 1792–1805 (2014)

Hongyan Zhang received the B.S. degree in geographic information system and the Ph.D. degree in photogrammetry and remote sensing from Wuhan University, China, in 2005 and 2010, respectively. He is currently an Associate Professor with the State Key Laboratory of Information Engineering in Surveying, Mapping, and Remote Sensing, Wuhan University. Dr. Zhang is a reviewer of about 10 international academic journals, and has published more than 30 research papers. His current research interests focus on image reconstruction, hyperspectral image processing, sparse representation, and low rank methods for sensing image imagery.

Liangpei Zhang (M'06–SM'08) received the B.S. degree in physics from Hunan Normal University, Changsha, China, in 1982, the M.S. degree in optics from the Chinese Academy of Sciences, Xian, China, in 1988, and the Ph.D. degree in photogrammetry and remote sensing from Wuhan University, Wuhan, China, in 1998. He is currently the Head of the Remote Sensing Division, State Key Laboratory of Information Engineering in Surveying, Mapping and Remote Sensing, Wuhan University. He is also a Chang-Jiang Scholar Chair Professor appointed by the Ministry of Education of China. He is currently a Principal Scientist for the China State Key Basic Research Project (2011–2016) appointed by the Ministry of National Science and Technology of China to lead the remote sensing program in China. He has more than 360 research papers. He is the holder of 15 patents. His research interests include hyperspectral remote sensing, high-resolution remote sensing, image processing, and artificial intelligence. Dr. Zhang is a Fellow of the Institution of Engineering and Technology, an Executive Member (Board of Governor) of the China National Committee of the International Geosphere-Biosphere Programme, and an Executive Member of the China Society of Image and Graphics. He regularly serves as a Cochair of the series SPIE Conferences on Multispectral Image Processing and Pattern Recognition, Conference on Asia Remote Sensing, and many other conferences. He edits several conference proceedings, issues, and Geoinformatics symposiums. He also serves as an Associate Editor of the International Journal of Ambient Computing and Intelligence, the International Journal of Image and Graphics, the International Journal of Digital Multimedia Broadcasting, the Journal of Geo-spatial Information Science, the Journal of Remote Sensing, and the IEEE TRANSACTIONS ON GEOSCIENCE AND REMOTE SENSING.

Huanfeng Shen (M'11–SM'13) received the B.S. degree in surveying and mapping engineering and the Ph.D. degree in photogrammetry and remote sensing from Wuhan University, Wuhan, China, in 2002 and 2007, respectively. In July 2007, he joined the School of Resource and Environmental Science, Wuhan University, where he is currently a full professor. His research interests include image processing (for quality improvement), remote sensing application, data fusion and assimilation. Dr. Shen has published more than 60 research papers. He has been supported by several talent programs, including the New Century Excellent Talents by the Ministry of Education of China (2011) and the Hubei Science Fund for Distinguished Young Scholars (2011).